

**Bi<sub>2</sub>Se<sub>3</sub> Sensitized ZnO Nanorod films for Improved Solar Cell Application**Ganga Shekar Pasupula<sup>1</sup>, R. S. Mane<sup>1</sup><sup>1</sup>Centre for Nanomaterials & Energy Devices, School of Physical Sciences, SRTM University, 431606 Nanded, India.**ABSTRACT:**

We report the synthesis of Bi<sub>2</sub>Se<sub>3</sub>/ZnO heterostructures by using chemical bath deposition method. The synthesized Bi<sub>2</sub>Se<sub>3</sub>/ZnO heterostructures have been characterized by X-ray diffraction (XRD), field emission scanning electron microscopy (FESEM), energy dispersive X-ray analysis (EDX), UV-Visible spectroscopy. The crystal structures of Bi<sub>2</sub>Se<sub>3</sub> and ZnO have been confirmed with crystallite sizes 18 nm and 26 nm respectively using XRD data. The nano particles (NPs) and nanorods (NR) like morphologies of Bi<sub>2</sub>Se<sub>3</sub> and ZnO have been observed by using FESEM. The elemental compositions have been investigated using EDX. The optical band gaps for Bi<sub>2</sub>Se<sub>3</sub>/ZnO and ZnO have been estimated to be 2.47 eV and 3.20 eV from UV-Visible analysis data. The ZnO and Bi<sub>2</sub>Se<sub>3</sub>/ZnO electrodes have been studied for the solar cell application. Current densities of bare ZnO and Bi<sub>2</sub>Se<sub>3</sub>/ZnO electrodes have been measured as 0.45 mA-cm<sup>-2</sup> and 1.45 mA-cm<sup>-2</sup> whereas power conversion efficiencies are 0.08% and 0.31% respectively. The electrochemical impedance spectroscopy (EIS) studies of solar cells have been carried out to study the charge transportation.

**Keywords** - Bi<sub>2</sub>Se<sub>3</sub>/ZnO, Heterostructures, CBD, Solar cells, Efficiency; FESEM.

**I. INTRODUCTION**

In recent years, the heterostructure solar cells with the combination of wide band gap metal oxide semiconductor as photo anode and narrow band gap semiconducting materials as photo sensitizer getting more attention. ZnO, one of the metal oxide semiconductors studied for various applications in the solar cells occupy an inevitable place as a photo anode in the solar cells because of its remarkable and beneficial properties such as good electrical conductivity, non-toxic, and low cost [1]. ZnO has wide band gap of the order of 3.37 eV with a large binding energy of 60 meV [2]. ZnO has potential applications in various fields such as piezoelectric materials [3], laser diodes [4], Gas sensors [5], Transistors [6], Ultraviolet detectors [7] and Solar cells [1]. Various nanostructures of ZnO have been reported such as nanoneedles [8], nanorods [9], nanotubes [10], and nanoflowers [2], so on.

So far several synthesis methods have been established for ZnO nanostructures such as Chemical bath deposition (CBD) [5], Hydrothermal [9], Successive ionic layer adsorption and reaction (SILAR) [11], Spray pyrolysis [12], Magnetron sputtering [8], and so on. Among these methods, SILAR and CBD methods have remarkable advantages such as easy processing, economical, large surface area deposition, good crystallinity, low cost and versatile method. Among various narrow band gap semiconducting photo sensitizer materials such as sulfides, and selenides, bismuth selenide (Bi<sub>2</sub>Se<sub>3</sub>) has recently gained much attraction in heterostructures solar cells device applications. Bi<sub>2</sub>Se<sub>3</sub> is a member of V-VI compound semiconductors family is a potential semiconducting material having optical band gap values in the range of 0.91 to 2.3 eV [13, 14]. The narrow band gap Bi<sub>2</sub>Se<sub>3</sub> semiconductor material has many applications in thermoelectric devices [15], photosensitive devices [14], photo-electrochemical (PEC) cells [16] and, so on. The Bi<sub>2</sub>Se<sub>3</sub> thin films have been synthesized by using various techniques, such as CBD [17], Spray pyrolysis [18], pulsed laser deposition [19], SILAR [20] and electro-deposition (ED) method [21]. Various nanostructures of Bi<sub>2</sub>Se<sub>3</sub> have been reported such as nanorods, and nanospheres [22], and nanoribbons [23], so on. As per our knowledge there is limited literature available on the preparation and characterization of semiconducting Bi<sub>2</sub>Se<sub>3</sub> in heterostructures solar cells. Present work on the deposition of narrow band gap semiconducting Bi<sub>2</sub>Se<sub>3</sub> on CBD deposited ZnO NRs film for improved solar cells performance is novel.

In the present work, ZnO NRs were grown on ITO substrate by seeding layer and CBD methods followed by synthesis of Bi<sub>2</sub>Se<sub>3</sub> photosensitization on ZnO electrodes. The electrode materials were characterized using standard materials characterization tools such as XRD, FESEM, EDX, and UV-Visible spectroscopy. The ZnO and Bi<sub>2</sub>Se<sub>3</sub>/ZnO electrodes were investigated for solar cells performance. The current density-voltage (J-V) characteristics were measured

for sandwich-type open cell using a flat platinum coated FTO plate as a counter electrode with polysulfide as liquid electrolyte. The electrochemical impedance (EIS) measurement of ZnO and Bi<sub>2</sub>Se<sub>3</sub>/ZnO electrodes was also performed for studying charge transportation.

## II. EXPERIMENTAL DETAILS

### 2.1. ZnO NRs Synthesis

Seeding layer method and double chemical bath deposition (CBD) methods were adopted to deposit ZnO NRs. Initially seeding layer was deposited by using 0.05M zinc nitrate (Zn(NO<sub>3</sub>)<sub>2</sub>·6H<sub>2</sub>O) solution in 25 mL double distilled water (DDW) as precursor. The pH of the precursor was maintained at ~10.5 by adding aqueous NH<sub>4</sub>OH (Ammonium Hydroxide) till the solution became clear at room temperature. The distilled water was taken in another beaker and kept at 89 °C in water bath. The ITO substrate was cleaned and dipped in Zn precursor solution (source of cations) for 45 s followed by 35 s dipping in distilled water (source of anions) beaker. In this way 15 cycles of dipping in both the solutions was carried out periodically and dried [24]. The light whitish colour was observed on ITO substrate which shows seeding layer formation. For the CBD of ZnO, similar clear Zn precursor solution was prepared and kept in water bath. The ITO substrate having seeding layer formation on it immersed in Zn precursor solution for 1 h at 89 °C [24-26]. A whitish colour was observed on ITO substrate. The ITO substrate was rinsed with distilled water and again kept for CBD deposition at 89 °C for 1 h. After double CBD process, a thick and dark whitish colour was appeared on ITO substrate. Final ITO substrate was rinsed with distilled water and air dried followed by air annealing at ~300 °C for 2 h.

### 2.2. Synthesis of Bi<sub>2</sub>Se<sub>3</sub> photosensitizers on ZnO deposited ITO electrode

For the deposition of Bi<sub>2</sub>Se<sub>3</sub> by CBD on ZnO deposited ITO electrode, bismuth nitrate (Bi(NO<sub>3</sub>)<sub>3</sub>·5H<sub>2</sub>O) and selenium powder were used as the sources for Bi and Se respectively. 0.05M bismuth nitrate was prepared in distilled water by adding optimized amount of HNO<sub>3</sub>, triethanolamine (TEA) and (sodium hydroxide) NaOH pellets to make clear solution (pH~12). Further 0.1M sodium seleno sulphite (Na<sub>2</sub>SeSO<sub>3</sub>) stock solution was prepared by adding selenium powder and sodium sulphite (Na<sub>2</sub>SO<sub>3</sub>) to 100 mL distilled water with stirring at 70 °C for 3 h. The Bi precursor and sodium seleno sulphite stock solutions were taken in 1:1 volumetric ratio in beaker and ZnO deposited ITO electrode was immersed and kept for 25 h at room temperature. The colour of solution turned to dark black. Substrate was taken out and rinsed with distilled water to remove loosely bond particles. The substrate was air dried followed by annealing at 200 °C for 1 h. Dark black colour was observed on final substrate electrode showing the formation of Bi<sub>2</sub>Se<sub>3</sub>. The obtained ZnO and Bi<sub>2</sub>Se<sub>3</sub>/ZnO electrodes were characterized and investigated for solar cell performance.

## III. RESULTS AND DISCUSSION

### 3.1. Structural Analysis

The structural investigation of the ZnO and Bi<sub>2</sub>Se<sub>3</sub> sensitized ZnO electrodes were performed by the X-ray diffraction (XRD). The XRD patterns were recorded by using an X-ray diffractometer with CuKα<sub>1</sub> radiations (λ=1.5406 Å) in 2θ range from 20-80 degree. The XRD patterns for Bi<sub>2</sub>Se<sub>3</sub>/ZnO deposited ITOs have been shown in Figure 1. Figure 1 shows the characteristic diffraction peaks of ITO as shown with asterisk (\*) [27]. The ZnO characteristics diffraction peaks for second electrode i.e. ZnO deposited ITO were observed at 31.45°, 34.43°, 36.27°, 47.53°, 62.87° and 72.56° which are represented by dot circle (●). The wurtzite (hexagonal) crystal structure of ZnO was confirmed by matching diffraction data with standard JCPDS data No: 36-1451. All the diffraction peaks are sharp and good intense which shows good crystallinity of obtained materials. The XRD peaks of third electrode i.e. Bi<sub>2</sub>Se<sub>3</sub>/ZnO electrode were observed at 25.06°, 29.36°, 33.79°, 43.63°, 56.59°, 66.41°, 67.92° and 69.15° which are associated with (101), (015), (107), (110), (1016), (1115), (0021) and (0120) crystal planes of Bi<sub>2</sub>Se<sub>3</sub>, respectively [JCPDS NO: 033-0214]. The highest XRD peak intensity of Bi<sub>2</sub>Se<sub>3</sub> was observed at 2θ = 56.56° corresponding to (1016) plane. The rhombohedral crystal structure of Bi<sub>2</sub>Se<sub>3</sub> was confirmed from XRD pattern. The average crystallite sizes of ZnO and Bi<sub>2</sub>Se<sub>3</sub> were calculated from the Scherer's formula,

$$D = \frac{K\lambda}{\beta \cos\theta} \quad (1)$$

Where K constant having value 0.9,  $\lambda$  is the X-ray wavelength (1.54 Å),  $\theta$  is the Bragg diffraction angle,  $\beta$  is the full width at half maximum. The crystallite sizes of the bare ZnO and Bi<sub>2</sub>Se<sub>3</sub> were determined as 26 nm and 18 nm respectively.

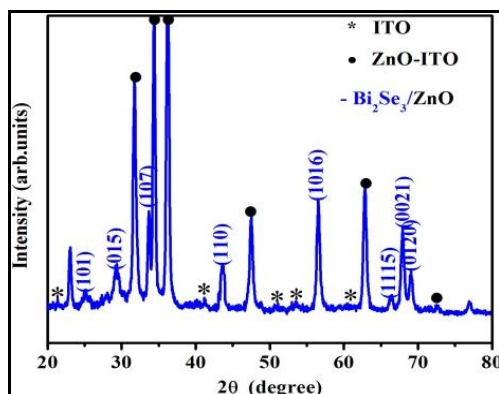


Figure 1. XRD patterns of Bi<sub>2</sub>Se<sub>3</sub>/ZnO-ITO electrodes.

### 3.2: Elemental Compositional Analysis

The elemental compositional analysis of Bi<sub>2</sub>Se<sub>3</sub>/ZnO hetero structure electrode was performed by energy dispersive X-ray (EDX) spectroscopy. The EDX spectrum has been shown in Figure 2. The presence of Zn, O, Bi and Se elements of Bi<sub>2</sub>Se<sub>3</sub>/ZnO hetero structure was confirmed from the EDX peaks. The weight and atomic percentages of all the elements have been shown in inset of Figure 2.

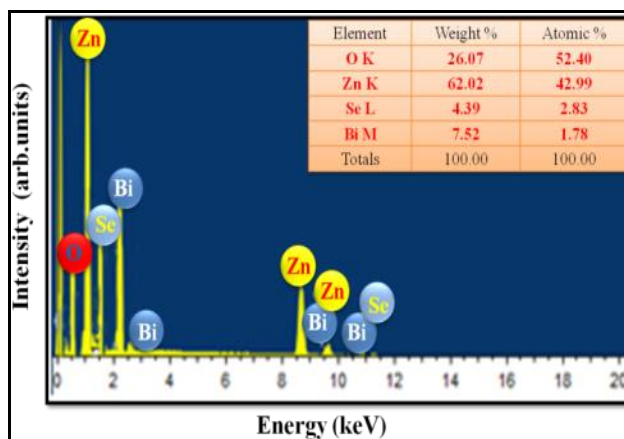


Figure 2. EDAX spectrum of Bi<sub>2</sub>Se<sub>3</sub>/ZnO-ITO electrodes

### 3.3. Morphological Analysis

FESEM analysis was carried out to study the morphology of ITO substrate, ZnO and Bi<sub>2</sub>Se<sub>3</sub>/ZnO electrodes. The FESEM images of all three samples (top view) have been shown in Figure 3. All the three FESEM images of three samples were recorded to confirm the deposition of ZnO and Bi<sub>2</sub>Se<sub>3</sub> materials separately and also to distinguish their morphologies. Figure 3(a) shows the spherical NPs like morphology of indium doped tin oxide (ITO). Figure 3 (b) shows the FESEM image of ZnO deposited on ITO substrate, with hexagonal NRs like morphology of ZnO. The ZnO NRs were randomly oriented having non uniform diameter and heights. NRs like morphology offer high surface area, high aspect ratio and also good continuity for charge transportation along NR length. This kind of morphology is favourable to solar cells device. Figure 3 (c) shows FESEM image of Bi<sub>2</sub>Se<sub>3</sub>/ZnO heterostructures electrode. In this image, mixed morphology of Bi<sub>2</sub>Se<sub>3</sub> and ZnO can be observed. The NPs like morphology was observed for Bi<sub>2</sub>Se<sub>3</sub> sample having non-uniform sizes which may be due to different growth of NPs at various sites on ZnO surface. The presence of Bi<sub>2</sub>Se<sub>3</sub> NPs on the top and in-between ZnO NRs gives good connectivity for charge transportation.

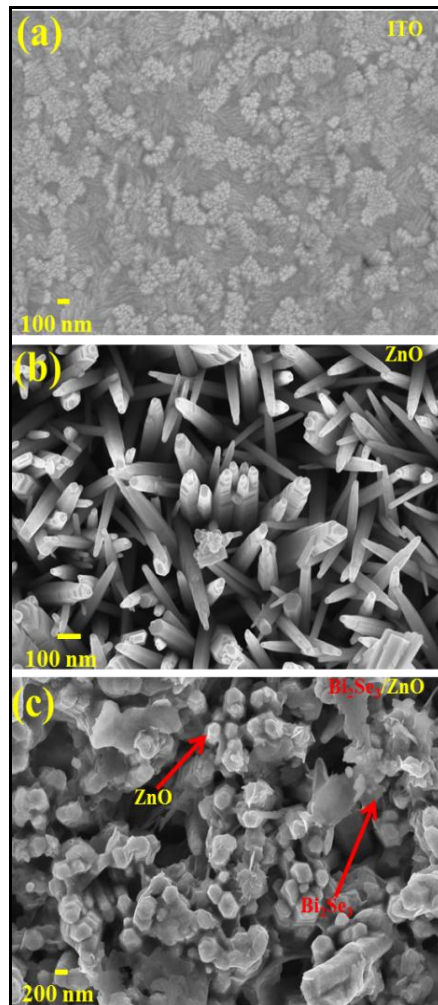


Figure 3. SEM images of (a) ITO substrate (b) ZnO nanorods on ITO substrate, (c) Bi<sub>2</sub>Se<sub>3</sub> sensitized ZnO electrode.

### 3.4. Optical Studies

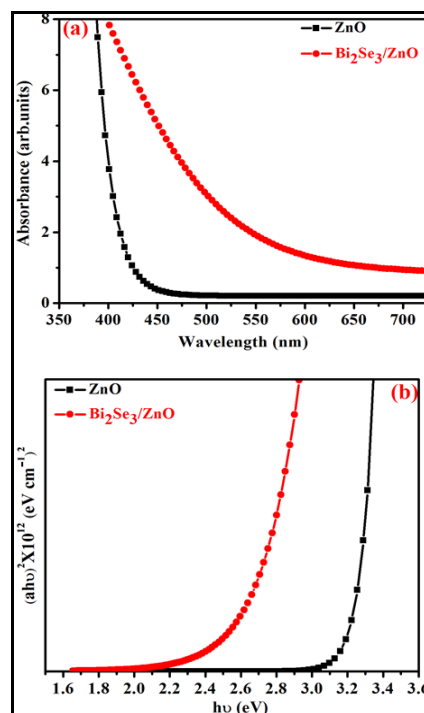


Figure 4. (a) UV-Visible absorbance spectra, (b) Energy band gaps of ZnO and Bi<sub>2</sub>Se<sub>3</sub>/ZnO-ITO electrodes.

The UV-Visible absorbance spectra of ZnO and Bi<sub>2</sub>Se<sub>3</sub>/ZnO samples were recorded and have been shown in Figure 4 (a). The absorbance peaks for both the samples lie near the edge of visible electromagnetic spectrum. The absorbance peak of Bi<sub>2</sub>Se<sub>3</sub>/ZnO sample shows red shift compared to ZnO which may attribute to the presence of Bi<sub>2</sub>Se<sub>3</sub> particles. The optical energy band gap values were estimated from Tauc's plot. The Tauc's relation of photon energy (hν) with absorption coefficient (α) is given as

$$\alpha = \frac{\alpha_0(h\nu - E_g)^n}{h\nu} \quad (2)$$

Where, E<sub>g</sub> = Energy band gap, α = absorption coefficient, α<sub>0</sub> = constant. The 'n' value depends on the type of transition. The 'n' has values 1/2. The Tauc's plots for both the samples have been shown in Figure 4 (b). The semiconducting nature absorption edge extrapolating the straight-line portion of the plot (αhν)<sup>2</sup> versus (hν) for zero absorption coefficient value gives the optical band gap (E<sub>g</sub>). The energy band gap values for ZnO and Bi<sub>2</sub>Se<sub>3</sub>/ZnO samples measured to be 3.20 and 2.47 eV respectively. The lower band gap value of Bi<sub>2</sub>Se<sub>3</sub>/ZnO sample may be attributed to the presence of narrow band gap Bi<sub>2</sub>Se<sub>3</sub> semiconducting material on ZnO NRs surface.

### 3.5. Photoelectrochemical Study

The current density and voltage (J-V) studies were carried out for ZnO and Bi<sub>2</sub>Se<sub>3</sub>/ZnO electrodes. The J-V characteristics for both the electrodes have been shown in Figure 5. The various solar cell performance parameters for the both electrodes were measured such as J-V, fill factor (FF) and efficiency (η) from the recorded data using their standard formulae. Solar cell parameters values for both the electrodes have been tabulated in Table 1. It was observed that the solar cell efficiency (0.31 %) value for Bi<sub>2</sub>Se<sub>3</sub>/ZnO heterostructures is higher than ZnO (0.08 %) electrode. This may be due to the higher number of photons absorbed by Bi<sub>2</sub>Se<sub>3</sub>/ZnO heterostructured materials which leads to number of electron hole pairs formations. This results into high number of charge carriers available for conduction/transportation and hence solar cell power efficiency. The Bi<sub>2</sub>Se<sub>3</sub>/ZnO heterostructure absorbs more photons due to low optical band gap as compared to ZnO. Hence, Bi<sub>2</sub>Se<sub>3</sub>/ZnO heterostructured electrode shows improved solar cell performance than ZnO.

**Table 1:** Parameters of bare ZnO and Bi<sub>2</sub>Se<sub>3</sub>/ZnO electrodes solar cell

Working electrode	V <sub>OC</sub> (V)	J <sub>s</sub> (mA-cm <sup>-2</sup> )	FF	η%
ZnO	0.29	0.45	0.62	0.08
Bi <sub>2</sub> Se <sub>3</sub> /ZnO	0.36	1.45	0.59	0.31

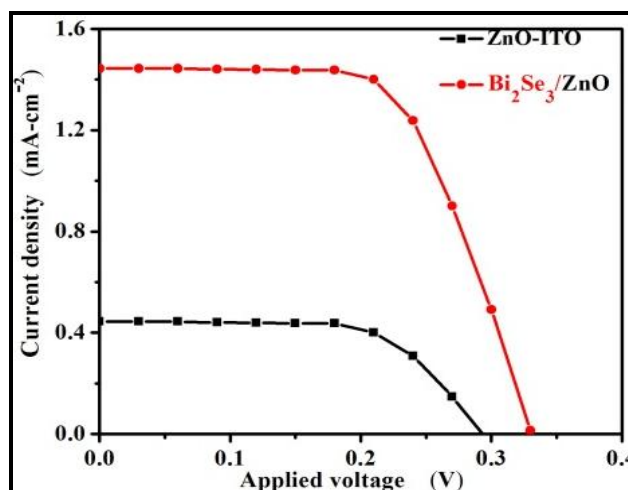


**Figure 5:** J-V analysis of ZnO-ITO and Bi<sub>2</sub>Se<sub>3</sub>/ZnO-ITO electrodes

### 3.6. Electrochemical Impedance Spectroscopy Study

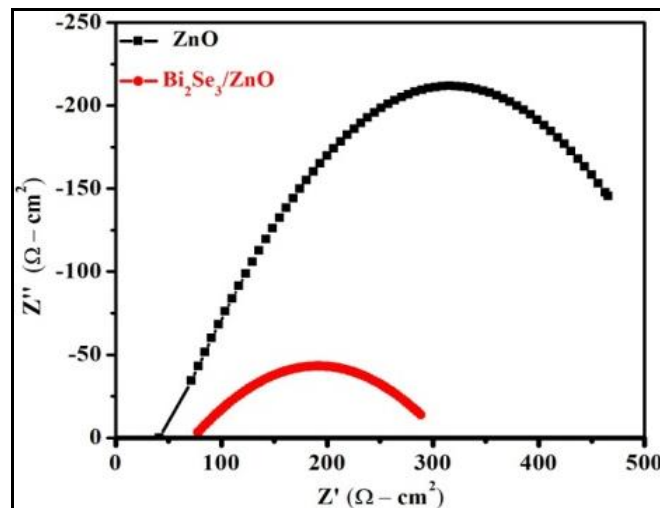


Figure 6. Impedance analysis of ZnO and Bi<sub>2</sub>Se<sub>3</sub>/ZnO-ITO electrodes.

The Electrochemical impedance spectroscopy studies of solar cells system for ZnO and Bi<sub>2</sub>Se<sub>3</sub>/ZnO electrodes were carried out by using EIS technique. The EIS Nyquist plots for both the electrode systems have been shown in Figure 6. The EIS study distinguishes the charge transport resistance and chemical capacitances of the solar cell device. The high and low frequency arcs in EIS correspond to the charge transport behaviour at counter electrode-electrolyte and electrolyte-photoanodes respectively.

## IV. CONCLUSIONS

In summary, ZnO NRs were grown on ITO substrate by seeding layer and CBD double deposition method. The Bi<sub>2</sub>Se<sub>3</sub> sensitization was carried out on ZnO NRs electrode surface to form heterostructures. The ZnO and Bi<sub>2</sub>Se<sub>3</sub>/ZnO heterostructures were characterized by standard materials characterization tools. Both the electrodes were investigated for solar cell performance. Current densities of ZnO and Bi<sub>2</sub>Se<sub>3</sub> sensitized ZnO electrodes were 0.45 mA-cm<sup>-2</sup> and 1.45 mA-cm<sup>-2</sup> whereas power conversion efficiencies were determined as 0.08% and 0.31 % respectively.

## REFERENCES

- [1] J.B. Baxter, A.M. Walker, K. van Ommering, E.S. Aydil, Synthesis and characterization of ZnO nanowires and their integration into dye-sensitized solar cells, *Nanotechnology*, 17 (2006) S304-S312.
- [2] Y. Liu, G. Han, Y. Li, M. Jin, Flower-like Zinc oxide deposited on the film of graphene oxide and its photoluminescence, *Mater. Lett.*, 65 (2011) 1885-1888.
- [3] M.P. Lu, J. Song, M.Y. Lu, M.T. Chen, Y. Gao, L.J. Chen, Z.L. Wang, Piezoelectric nanogenerator using p-type ZnO nanowire arrays, *Nano Lett.*, 9 (2009) 1223-1227.
- [4] D.C. Reynolds, D.C. Look, B. Jogai, Optically pumped ultraviolet lasing from ZnO, *Solid State Commun.*, 99 (1996) 873-875.
- [5] C.D. Lokhande, P.M. Gondkar, R. S. Mane, V.R. Shinde, Sung-Hwan Han, CBD grown ZnO-based gas sensors and dye-sensitized solar cells, *J. of Alloys and Compounds*, 475 (2009) 304-311.
- [6] E. Fortunato, P. Barquinha, A. Pimentel, A. Goncalves, A. Marques, L. Pereira, R. Martins, Recent advances in ZnO transparent thin film transistors, *Thin Solid Films*, 487 (2005) 205-211.
- [7] Y. Liu, C.R. Gorla, S. Liang, N. Emanetoglu, Y. Lu, H. Shen, M. Wraback, Ultraviolet detectors based on epitaxial ZnO films grown by MOCVD, *J. Electron. Mater.*, 29 (2000) 69-74.
- [8] S. Kumar, V. Gupta, K Sreenivas, Synthesis of photo conducting ZnO nano-needles using an unbalanced magnetron sputtered ZnO/Zn/ZnO multilayer structure, *Nanotechnology*, 16 (2005) 1167-1171.
- [9] Y.F. Hsu, Y.Y. Xi, A.B. Djuricic, W.K. Chan, ZnO nanorods for solar cells: Hydrothermal growth versus vapor deposition, *Appl. Phys. Lett.*, 92 (2008) 133507.

- [10] H. Yu, Z. Zhang, M. Han, X. Hao, F. Zhu, A general low-temperature route for large-scale fabrication of highly oriented ZnO nanorod/nanotube arrays, *J. Am. Chem. Soc.*, 127 (2005) 2378–2379.
- [11] P. Suresh Kumar, A. Dhayal Raj, D. Mangalaraj, D. Nataraj, Growth and characterization of ZnO nanostructured thin films by a two-step chemical method, *Applied Surface Science*, 255 (2008) 2382–2387.
- [12] U.T. Nakate, P. Patil, R.N. Bulakhe, C.D. Lokhande, S.N. Kale, M. Naushad, R.S. Mane, Sprayed zinc oxide films: Ultra-violet light-induced reversible surface wettability and platinum-sensitization-assisted improved liquefied petroleum gas response, *J. Coll. Interfaces Sci.*, 480 (2016) 109-117.
- [13] S. Augustine, S. Ampili, J. K. Kang, E. Mathai, Structural, electrical and optical properties of Bi<sub>2</sub>Se<sub>3</sub> and Bi<sub>2</sub>Se<sub>(3-x)</sub>Te<sub>x</sub> thin films, *Mater. Res. Bull.*, 40 (2005) 1314-1325.
- [14] X. Yang, X. Wang, Z. Zhang, Synthesis and optical properties of single-crystalline bismuth selenide nanorods via a convenient route, *J.Cryst. Growth*, 276 (2005) 566-570.
- [15] K. Kadel, L. Kumari, W. Z. Li, J. Y. Huang and P. P. Provencio, Synthesis and Thermoelectric Properties of Bi<sub>2</sub>Se<sub>3</sub> Nanostructures, *Nanoscale Res. Lett.*, 6 (2011) 57-64.
- [16] S. D. Kharade, N. B. Pawar, V. B. Ghanwat, S.S. Mali, W. R. Bae, P.S. Patil, C.K. Hong, J.H. Kim, P.R.N. Bhosale, Room temperature deposition of nanostructured Bi<sub>2</sub>Se<sub>3</sub> thin films for photo electrochemical application: effect of chelating agents, *New J. Chem.*, 37 (2013) 2821-2828.
- [17] C.D. Lokhande, B.R.Sankapal, R.S.Mane, H.M. Pathan, M.Muller, M.Giersig, H.Tributsch, V.Ganeshan, Structural characterization of chemically deposited Bi<sub>2</sub>S<sub>3</sub> and Bi<sub>2</sub>Se<sub>3</sub> thin films, *Applied Surface Science*, 187 (2002) 108-115.
- [18] H.D. Li, L. Gao, H. Li, G.Y. Wang, J. Wu, Z.H. Zhou, Z.M. Wang, Growth and band alignment of Bi<sub>2</sub>Se<sub>3</sub> topological insulator on H-terminated Si(1 1 1) vander Waals surface, *Appl. Phys. Lett.*, 102 (2013) 74106.
- [19] Lijian Meng, Hui Meng, Wenjie Gong, Wei Liu and Zhidong Zhang, Growth and characterization of Bi<sub>2</sub>Se<sub>3</sub> thin films by pulsed laser deposition using alloy target, *Thin Solid Films*, 519 (2011) 7627-7631.
- [20] B.R. Sankapal, C.D. Lonkhande, Photo electrochemical characterization of Bi<sub>2</sub>Se<sub>3</sub> thin films deposited by SILAR technique, *Mater. Chem. Phys.*, 73 (2002) 151-155.
- [21] A.P. Torane, C.D. Lokhande, P.S. Patil, and C.H. Bhosale, Preparation and characterization of electrodeposited Bi<sub>2</sub>Se<sub>3</sub> thin films, *Mater. Chem. Phys.*, 55 (1998) 51-54.
- [22] Shu Xu, Wen-bo Zhao, Jian-Min Hong, Jun-Jie Zhu, Hong-Yuan Chen, Photochemical synthesis of Bi<sub>2</sub>Se<sub>3</sub> nanosphere and nanorods, *Materials Letters*, 59 (2005) 319 – 321.
- [23] H. Tang, D. Liang, R.L.J. Qiu, X.P.A. Gao, Two-dimensional transport-induced linear magneto-resistance in topological insulator Bi<sub>2</sub>Se<sub>3</sub> nanoribbons, *ACS Nano*, 5 (2011) 7510–7516.
- [24] P. S. Kumar, P. Paik, A. D. Raj, D. Mangalaraj, D. Nataraj, A. Gedanken, S. Ramakrishna, Biodegradability study and pH influence on growth and orientation of ZnO nanorods via aqueous solution process, *Applied Surface Science*, 258 (2012) 6765– 6771.
- [25] P.K. Baviskar, P.R. Nikam, S.S. Rao Gargote, Ahmed Ennaoui, B.R. Sankapal, Controlled synthesis of ZnO nanostructures with assorted morphologies via simple solution chemistry, *J. Alloys Comp.*, 551 (2013) 233–242.
- [26] R. S. Mane, W. J. Lee, C.D. Lokhande, B. W. Cho, S. H. Han, Controlled repeated chemical growth of ZnO films for dye-sensitized solar cells, *Current Applied Physics*, 8 (2008) 549–553.
- [27] S. Jana, P. Mondal, S. Tripathi, A. Mondal, B. Chakraborty, Electrochemical synthesis of FeS<sub>2</sub> thin film: An effective material for peroxide sensing and terephthalic acid degradation, *J. Alloys. Comp.*, 646 (2015) 893-899.